Observation of the Hydration-Dependent Conformation of the $(dG)_{20}$•$(dG)_{20}(dC)_{20}$ Oligonucleotide Triplex Using FTIR Spectroscopy†

A. P. White and J. W. Powell*

Department of Physics, Reed College, 3203 Southeast Woodstock Boulevard, Portland, Oregon 97202

Received November 30, 1994®

ABSTRACT: The triple-helical oligonucleotide $(dG)_{20}$•$(dG)_{20}(dC)_{20}$ was investigated using FTIR spectroscopy. Mid-infrared spectra were collected at nine relative humidities (RH) between 0% and 98%. The highest humidity spectrum agrees with the solution spectrum of a polynucleotide $(dG)_n$•$(dG)_n(dC)_n$ triplex [Ouali, M., Letellier, R., Sun, J. S., Akhebat, A., Adnet, F., Liquier, J., & Taillandier, E. (1993) *J. Am. Chem. Soc. 115,* 4264−4270]. A dramatic transition in the vibrational state of the molecule has been observed between 88% and 92% RH. Theoretical predictions concerning the effects of hydration on a (dG)•(dG)-(dC) oligonucleotide triplex [Laughton, C. A., & Neidle, S. (1992) *Nucleic Acids Res. 20,* 6535−6541; Mohan, V., Smith, P. E., & Pettitt, M. B. (1993) *J. Am. Chem. Soc. 115,* 9297−9298] have been considered and compared to our results. The infrared marker bands for the conformation of the glycosidic bond are absent below 92% RH, although dramatic hydration-dependent vibrational changes have been observed in the spectral regime traditionally associated with the glycosidic linkages. The effect of water in the Watson−Hoogsteen groove upon the vibrational state of the triplex has been observed for the first time. Hydration-induced changes in vibrational state have also been observed in the base residues, the phosphodiester backbone, and the furanose rings of the oligonucleotide sample.

Although the nucleic acid triplex was discovered in 1957 (Felsenfeld *et al.,* 1957), it was not until recently that significant triple-stranded research activity transpired. A resurgence of interest in the triple-stranded structure was stimulated by the realization that the triplex offered viable biochemical and pharmacological applications. The high specificity with which a third strand oligonucleotide binds to an associated duplex (Moser & Dervan, 1987) provides a powerful artificial endonuclease (François *et al.,* 1989; Strobel & Dervan, 1991) when the third strand is coupled with a cleaving agent. It has been shown that this activity holds strong promise for applications such as genome mapping (Strobel *et al.,* 1991). The site-specific character of triplex formation also holds promise in therapeutic applications. Oligonucleotide-directed triple-helix formation in a gene's promoter region has been shown to downregulate the expression of that gene through the inhibition of mRNA synthesis (Cooney *et al.,* 1988; Duval-Valentin *et al.,* 1992; Grigoriev *et al.,* 1992; Maher *et al.,* 1992). The intermolecular triplex has recently been shown to inhibit gene expression *in vivo* (Ing *et al.,* 1993), including a case demonstrating the inhibition of HIV-1 transcription in infected human cells (McShan *et al.,* 1992). Medically related issues such as these have been vigorous motivators of triple-stranded research in the past five years.

Significant progress has been made in understanding characteristics of the triplex as a gene control tool. The ability to design oligonucleotides which will recognize any unique base pair sequence and form a stable triplex in a promoter region of the human genome, however, still remains a challenge. In general, the stable triplex structure has been restricted to a homopurine−homopyrimidine duplex in which the additional third strand binds to the homopurine strand of the duplex. In order to extend this third strand binding to any random base pair sequence, comprehension of the microscopic parameters necessary for the stability of triple-stranded systems is crucial. The interaction of the triplex with water molecules is a central issue of stability, as mainly evidenced by two results. First, a spine of hydration in duplex DNA increases its stability, as seen by the corroboration of melting data and the modified self-consistent phonon approximation theory (Chen & Prohofsky, 1994a). Second, a molecular dynamics simulation has recently predicted the existence of a spine of water molecules bonding the amino protons of the cytosine and guanine residues in the Watson−Hoogsteen groove of a $(dG)_7$•$(dG)_7(dC)_7$ oligonucleotide triplex (Mohan *et al.,* 1993). An experimental investigation using NMR spectroscopy has also identified hydration sites in a R•RY DNA triplex (Radhakrishnan & Patel, 1994b). Possible binding sites for long-lived water molecules were found in both the Crick−Hoogsteen and the Watson−Hoogsteen grooves of the molecule. A molecular mechanics model has been used recently to predict hydration-dependent characteristics of a $(dG)_{10}$•$(dG)_{10}(dC)_{10}$ triplex (Laughton & Neidle, 1992). This calculation predicted two likely structures. First, when a distance-dependent dielectric constant was used to mimic the shielding effect of solvent, the third strand is reverse Hoogsteen hydrogen bonded with *syn* guanine residues. When explicit solvent molecules were included in the calculation, however, the structure's third strand is Hoogsteen bonded with *anti* guanine residues. Studies such as these will contribute to the atomic level understanding of the triplex system, which is necessary for successful applications in the realm of gene control.

FTIR spectroscopy is well-suited to identify the hydration-dependent character of the triplex since (1) the spectroscopic

† This work was supported by the National Science Foundation DMB 90107105 and by a grant from the Howard Hughes Medical Institute made to Reed College under the 1991 Undergraduate Biological Sciences Initiative.

* To whom correspondence should be addressed.

® Abstract published in *Advance ACS Abstracts,* January 15, 1995.

0006-2960/95/0434-1137$09.00/0

signatures of the above-mentioned structures have been published recently, and (2) the technique for varying hydration from vacuum conditions to the desired number of water molecules per nucleotide are well-established (Lindsay *et al.*, 1988). We have studied a $(dG)_{20}$•$(dG)_{20}(dC)_{20}$ oligonucleotide triplex in nine relative humidity (RH)[1] environments. The third strand of the sample (Pu•) is bound antiparallel, through Hoogsteen hydrogen bonds, to the purine strand of a Watson–Crick duplex and lies in its major groove. The $(dG)_{20}$•$(dG)_{20}(dC)_{20}$ oligonucleotide triplex is of the purine•purine–pyrimidine motif (Pu•PuPy) and will be denoted G•GC where the '•' indicates the location of the Hoogsteen bond. The third purine strand will be referred to as the Hoogsteen strand, while the purine and pyrimidine strands of the duplex will be referred to as the Watson and Crick strands, respectively. The three grooves of the triplex will be referred to here as Watson–Crick, Crick–Hoogsteen, and Watson–Hoogsteen in relation to the bonding scheme between the two strands which define each groove. Although study of this Pu•PuPy motif has not been as extensive as study of the Py•PuPy motif, the G•GC system was chosen for its ease and reliability of formation from single-stranded oligonucleotides.

MATERIALS AND METHODS

$(dG)_{20}$•$(dG)_{20}(dC)_{20}$ Preparation. Samples of three 20-mer oligonucleotides [$(dG)_{20}$ (sequence name G07454), $(dG)_{20}$ (sequence name G07455), and $(dC)_{20}$ (sequence name C06461)] were synthesized by Macromolecular Resources. The 11.0-μmol samples were RP-1 purified. Triplex formation was performed first by equimolar mixing of $(dG)_{20}$ and $(dC)_{20}$, each in buffered salt solution (0.1 mM EDTA and 50 mM NaCl) at 90 °C to prohibit interstrand aggregation (Plum *et al.*, 1990). The sample was slowly annealed (10 °C/h) past the double-stranded T_m (65 °C) to establish the formation of the $(dG)_{20}(dC)_{20}$ duplex. Equimolar mixing of the de-aggregated third $(dG)_{20}$ strand and the duplex at 60 °C followed by slow annealing (10 °C/h) past the triple-stranded T_m (35 °C) formed the $(dG)_{20}$•$(dG)_{20}(dC)_{20}$ triplex.

The hyperchromic effect was utilized to confirm triplex-helix formation. Ultraviolet absorption at 260 nm was monitored with increasing temperature. The triple-stranded to double-stranded phase transition was observed at 37 °C, and the double-stranded to single-stranded phase transition was observed at 67 °C. Phase transitions observed in these temperature regimes reliably confirmed the formation of the G•GC oligonucleotide triplex.

Samples were hydrated, always with an incremental increase in water content, by exposing the nucleic acid films to environments of different relative humidities long enough to ensure equilibration of each consecutive hydration state. The film of the $(dG)_{20}$•$(dG)_{20}(dC)_{20}$ sample was hydrated within desiccators for 24 h between each level of hydration. It was previously determined that water absorption (near 700 cm^{-1}) was proportional to equilibration time for up to 6 h, while equilibration times over 24 h did not have any significant effect upon sample water content. Constant humidity levels were established and regulated within the desiccators by the continual exchange of water molecules between the air and a saturated salt solution at constant room temperature. The relative humidity levels and associated salts utilized in the experiments are as follows: 33%, $MgCl_2$; 58%, NaBr; 66%, $NaNO_2$; 75%, NaCl; 81%, $(NH_4)_2SO_4$; 88%, K_2CrO_4; 92%, $Na_2C_4H_4O_6$•$2H_2O$; and 98%, $CaSO_4$. A relative humidity meter (Fischer Scientific) was used to experimentally confirm relative humidity and temperature within the desiccators.

Spectroscopy. Hydrated films were placed in a sealed sample cell, which maintained the proper relative humidity during spectroscopy. Relative humidities were maintained within the air-tight mid-infrared transparent sample cell by the presence of an appropriate saturated salt solution or desiccating agent. Samples of the G•GC oligonucletide were applied directly to the sample cell's ZnSe window.

Infrared spectroscopy was performed at room temperature on a Bruker 113v Fourier transform infrared spectrometer. The Fourier transform of the interferogram of the sample plus sample cell was divided by the Fourier transform of the interferogram of the sample cell (reference) for each relative humidity. Typically 300 scans of sample and reference were taken. The active element of the detector was DTGS at room temperature. The original spectra are presented here; no Fourier deconvolutions or subtractions have been performed.

RESULTS

Our results are presented in Figures 1–4. The spectra of the sample for nine relative humidities are presented, each in a different frequency regime. These spectra have been vertically shifted in absorption units for ease of presentation; appropriate constants have been added to each of the spectra to allow for convenient comparison between adjacent hydration states. The scale of absorption intensity is preserved for the spectra in each figure, and the intensity of a typical absorption is reported in each figure legend. The most relevant absorption peaks are labeled with their peak frequencies for purposes of discussion.

DISCUSSION

In the mid-infrared, the interval from 800 to 1000 cm^{-1} corresponds to stretching vibrations of the furanose sugar ring as well as vibrations in the sugar ring which are coupled to atomic vibrations of the adjacent phosphate group. Between 1000 and 1250 cm^{-1}, vibrations of the backbone phosphate groups absorb radiation. The region from 1250 to 1500 cm^{-1} represents the vibrations of the glycosidic bonds as well as several stretching vibrations of the nitrogenous bases. The higher frequencies between 1500 and 1800 cm^{-1} are those of the in-plane double-bond vibrations of the bases. Molecular structural features can be derived from the spectroscopic character of each of these regions. This preliminary report will present the spectral data and discuss the most significant results from each of the four spectral regimes.

Furanose Frequency Region. The spectra in the 800–1000 wavenumber region are exhibited in Figure 1. The absorptions at 802 cm^{-1} in the lower relative humidity spectra are due to sugar ring vibrations and are markers for the C3′-*endo* sugar pucker. The 802-cm^{-1} peak is relatively weak in the spectra of the sample at higher hydration states due to the strong and broad water absorptions around 800 cm^{-1}. A mode at 815 cm^{-1}, which is completely absent at 0% and 33% RH is evident at 58% RH. These two vibrations, together with the 865-cm^{-1} mode, which are present in all

[1] Abbreviations: relative humidity, RH; $(dG)_{20}$•$(dG)_{20}(dC)_{20}$, G•GC.

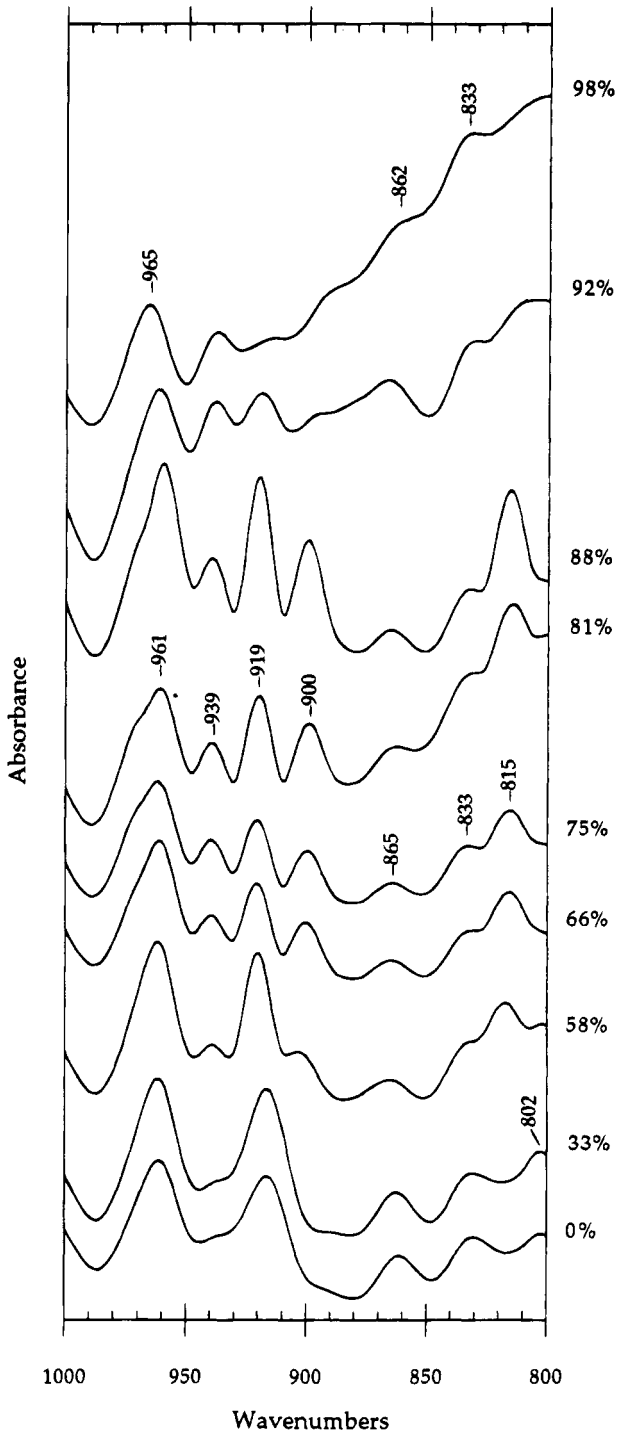

FIGURE 1: Absorption spectra of the hydration series of the $(dG)_{20}$·$(dC)_{20}(dG)_{20}$ oligonucleotide triplex in the range from 800 to 1000 cm^{-1}. The absorption of the nominal 961-cm^{-1} band at 0% RH is 0.67 absorption unit. The x-axis for the 0% spectrum represents an absorption of 0.45 absorption unit.

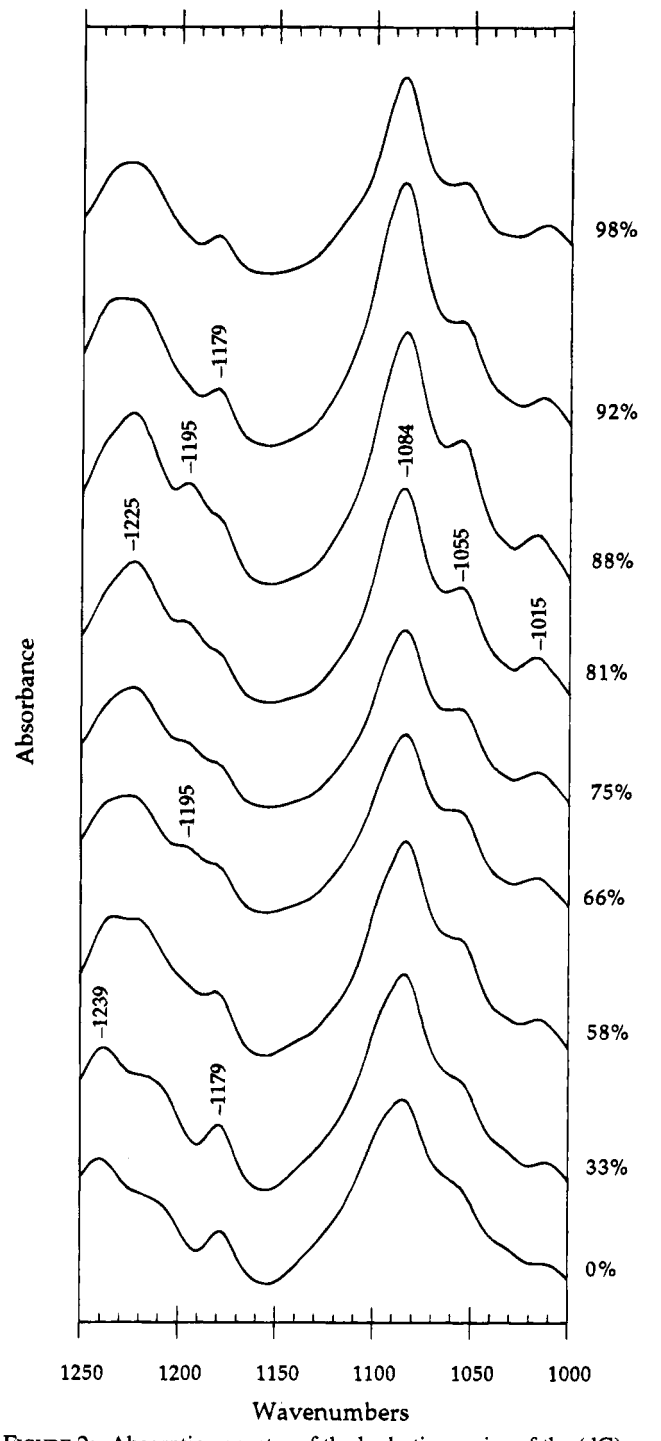

FIGURE 2: Absorption spectra of the hydration series of the $(dG)_{20}$·$(dC)_{20}(dG)_{20}$ oligonucleotide triplex in the range from 1000 to 1300 cm^{-1}. The absorption of the 1084-cm^{-1} band at 0% RH is 1.07 absorption units. The x-axis for the 0% RH spectrum represents an absorption of 0.45 absorption unit.

hydration states, are indicative of the C3′-*endo* geometry of the furanose ring. The conformationally sensitive mode which exists nominally at 833 cm^{-1} is a marker band for the C2′-*endo* geometry of the furanose ring (Taillandier *et al.*, 1985). This vibration has been observed in similar triple-stranded samples (Akhebat *et al.*, 1992). The 833-cm^{-1} mode occurs in double-stranded DNA at high hydration states, and the fact that this band persists with strong oscillator strength in all hydration states is evidence for a robust spine of hydration. Thus, there are vibrational contributions from two sugar puckers in the $(dG)_{20}$·$(dG)_{20}$-$(dC)_{20}$ triplex. This phenomenon has been previously observed in triplex samples whose Watson–Crick bound strands include an RNA strand (Liquier *et al.*, 1991). Based on the relative intensities of pucker marker bands in a polynucleotide G·GC triplex in solution, it has been proposed that the dC strand has C2′-*endo* sugar puckers while both of the dG strands have C3′-*endo* geometry (Ouali *et al.*, 1993).

Backbone Frequency Region. Figure 2 depicts the spectra of the G·GC oligonucleotide at the nine hydration states between 1000 and 1250 cm^{-1}. The most prominent band at 1084 cm^{-1} has long been known to be due to the symmetric

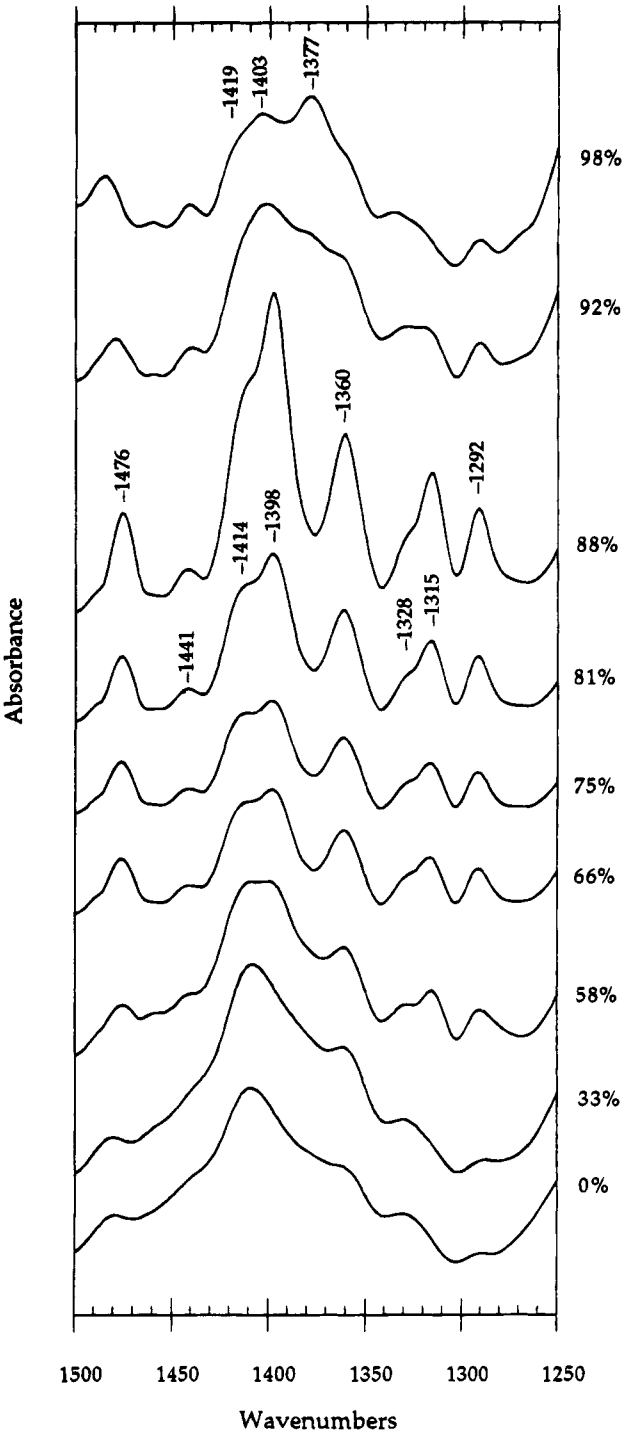

FIGURE 3: Absorption spectra of the hydration series of the $(dG)_{20}$·$(dC)_{20}(dG)_{20}$ oligonucleotide triplex in the range from 1200 to 1500 cm^{-1}. The absorption of the 1476-cm^{-1} band at 0% RH is 0.75 absorption unit. The *x*-axis for the 0% RH spectrum represents an absorption of 0.45 absorption unit.

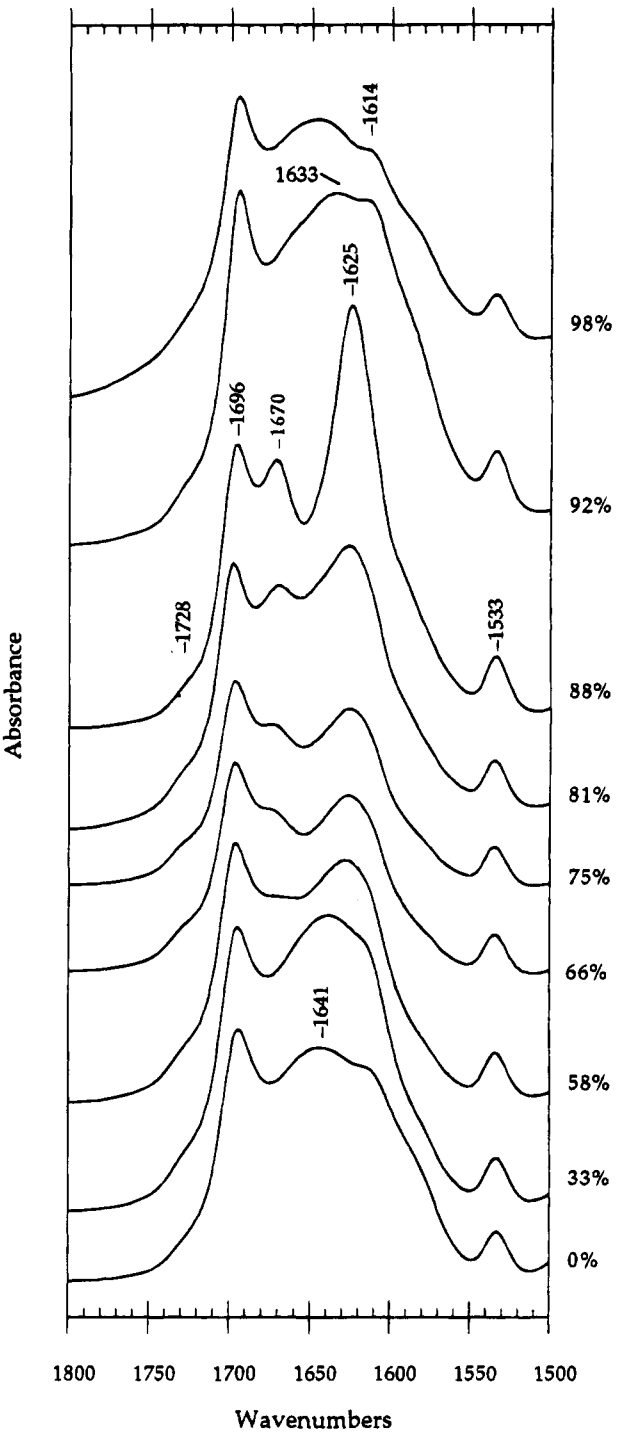

FIGURE 4: Absorption spectra of the hydration series of the $(dG)_{20}$·$(dC)_{20}(dG)_{20}$ oligonucleotide triplex in the range from 1500 to 1800 cm^{-1}. The absorption of the nominal 1696-cm^{-1} band at 0% RH is 1.46 absorption units. The *x*-axis for the 0% RH spectrum represents an absorption of 0.45 absorption unit.

PO_2^- vibration coupled with the C5′−O5′ stretch (Taillandier *et al.*, 1985). This spectral characteristic is the backbone evidence of the B-type conformation.

The absorption which shifts in frequency with hydration from 1239 cm^{-1} at 0% RH to 1225 cm^{-1} at 88% RH is conformationally sensitive. The 1239-cm^{-1} mode indicates the presence of the A-type molecular conformation in the backbone while the 1225-cm^{-1} absorption is a marker band for the B-type conformation (Simanouchi *et al.*, 1964). As with the furanose region, components of both conformations are apparent throughout the hydration series.

The band at 1179 cm^{-1}, which is present in all hydration states but most apparent in the two extremes of relative humidity, is assigned to a deoxy C3′-*endo*/*anti* vibration (Sfihi *et al.*, 1993). Thus, there is a C3′-*endo*/*anti* component to the G·GC sample throughout the range of relative humidities and especially in the lowest (0%, 33%) and in the highest (92%, 98%) hydration states. The observation of this vibrational mode agrees with the observations of vibrational state made in both the furanose and glycosidic regimes.

Glycosidic Bond Frequency Region. In Figure 3, the spectral region between 1250 and 1500 wavenumbers, the glycosidic bond absorptions are displayed. The bond conformation can be determined by analysis of these absorptions. The traditional marker band for the glycosidic bond vibration in the *syn* conformation is 1355 cm^{-1}, while in the *anti* conformation it is 1376 cm^{-1} (Taboury *et al.*, 1985). Neither of these absorptions are recognizable in the sample at lower relative humidities. At higher hydration states, however, a vibration at 1377 cm^{-1} becomes apparent, indicating the *anti* conformation of the glycosidic linkage. This absorption together with the bands observed at 1403 and 1419 cm^{-1} matches those observed in the glycosidic regime (Ouali *et al.*, 1993) for a polynucleotide G·GC sample in solution.

C. A. Laughton and S. Neidle have performed molecular modeling calculations to predict the glycosidic bond conformation (Laughton & Neidle, 1992). Their studies predict that the conformation is *anti* if polar solvent molecules are included in the calculation and that the bond conformation is *syn* if the calculation is performed with a dielectric constant mimicking the shielding effects of water. The vibrational observations made here of the G·GC oligonucleotide system show that the conformation of the glycosidic bond is *anti* in the higher solution-like hydration states. To our knowledge, vibrational evidence of the *syn* conformation is absent, and the conformation of the glycosidic linkages in solution is *anti*.

The band at 1414 cm^{-1} is associated with the glycosidic linkage of the guanosine nucleoside (N9-C8 with H-C2′-H and C5-N7) (Letellier *et al.*, 1986) and has been observed both in samples whose conformations were C3′-*endo*/-*anti* and in samples whose conformations were C3′-*endo*/-*syn* (Sfihi *et al.*, 1993). In Figure 3 as relative humidity increases from 88% RH, the 1414-cm^{-1} band becomes a shoulder to the strong band at 1398 cm^{-1}. This 1398-cm^{-1} band, which appears to be the 1403-cm^{-1} mode downshifted in frequency, is assigned to the coupling of the guanosine imidazole ring and sugar deformations (Ouali *et al.*, 1993). The extreme increase in the band width of modes between 1315 and 1415 cm^{-1} characterizes the dramatic phase transition which occurs in the triplex between 88% and 92% RH.

The strong band at 1360 cm^{-1} is assigned to the coupling of the amino group of the cytosine base residue to the phosphodiester backbone, through the furanose ring (H-C3′-O3′, C6-NH_2 and N1C1′H) (Letellier *et al.*, 1986). This band increases with relative humidity until 88%, after which it returns to a vibrational state with lower absorption. The oscillator strength of the cytosine amino absorption, which is a component of this hydration-dependent mode at 1360 cm^{-1}, may be increasing with hydration state due to interactions with water molecules in the Watson−Hoogsteen groove of the triplex.

Base Residue Frequency Region. The mid-infrared region from 1500 to 1800 wavenumbers in Figure 4 generally represents the in-plane double-bond vibrations and the high-frequency vibrations of the nucleic acid bases. These vibrations are sensitive to base interactions such as base stacking and base pairing. Helical stability, induced by the interaction of water molecules with the hydrophobic bases, can also be inferred from the base interaction-dependent vibrations. Evidence of the theoretically predicted spine of hydration in the Watson−Hoogsteen groove can be seen in this region and is discussed below.

The band at 1476 cm^{-1} is associated with the guanine base residue. It increases in oscillator strength with increasing relative humidity. This band depends strongly upon the C8-H bending vibration in guanine (Sfihi *et al.*, 1993). The dipole moment of the C8-H pair increases with the association of a polar water molecule. As hydration increases, the oscillator strength of this bending vibration also increases as more and more guanine residues interact with available water molecules.

The marker bands for the Hoogsteen-bound bases are found in this frequency regime and will be used to confirm triple strandedness. The strong absorption at 1696 cm^{-1} and the shoulder above 1700 cm^{-1} are evidence of the interaction of the third strand with the Watson−Crick duplex. The strongest component of the 1696-cm^{-1} mode is the C6=O6 stretching vibration in the guanine residues. With the formation of a G·GC triplex, this band is shifted from 1689 cm^{-1} in a polynucleotide $(dG)_n(dC)_n$ duplex to 1696 cm^{-1} in a polynucleotide $(dG)_n{\cdot}(dG)_n(dC)_n$ triplex (Ouali *et al.*, 1993). A new absorption above 1700 cm^{-1} appears which corresponds to a carbonyl vibration coupled by Hoogsteen bonding to complementary base vibrations (Liu *et al.*, 1993). This unusually high wavenumber absorption at 1728 cm^{-1} is a Hoogsteen marker band and indicates the presence of a third strand binding scheme (Taillandier & Liquier, 1992).

Water-mediated changes in the vibrational state of the triplex are evidenced by the increase in oscillator strength of both the 1670- and the 1292-cm^{-1} mode. These vibrations, which are associated with the amino group of the cytosine base residue, demonstrate the presence of water in the Watson−Hoogsteen groove of the molecule. The absorption at 1670 cm^{-1} is the marker band of the cytosine C6-NH_2 bending vibration, and the band at 1292 cm^{-1} is representative of the cytosine C6-NH_2 stretching vibration (Tsuboi *et al.*, 1962). The interaction of a polar water molecule with the cytosine amino group increases the dipole moment of the amino group and, thus, increases the oscillator strength of both the stretching and bending modes. As the hydration state increases and the number of sample nucleotides with water bound in the Watson−Hoogsteen spine of hydration increases, the strength of the cytosine C6-NH_2 vibrations increases. This observation corroborates the molecular dynamics prediction of Pettitt and co-workers (Mohan *et al.*, 1993) that a series of water molecules are bound between the cytosine amino group and the third strand guanine amino group in the Watson−Hoogsteen groove of the helix.

The absorption at 1696 cm^{-1} has vibrational contributions from both the C6=O6 stretch coupled to a guanine ring vibration and the stretching and scissoring modes of the guanine amino group (Ghomi & Taillandier, 1985). The strong absorption of the carbonyl group, which is attributed to its large dipole moment, makes it difficult to determine the contribution of the amino group vibrations in this mode. The prediction that a spine of hydration exists which binds the amino groups of the guanine and cytosine bases (Mohan *et al.*, 1993) is then difficult to evaluate with respect to the vibrational state of the guanosine amino group.

CONCLUSIONS

In the G·GC oligonucleotide triplex, a dramatic structural and dynamical transition has been found between 88% and

92% RH, as seen most prominently in Figures 3 and 4. Utilizing gravitimetric measurements of double-stranded DNA complexed with water (Lindsay *et al.*, 1988), we have made some preliminary estimations of the number of water molecules per triplex nucleotide at each hydration state. The plot of g of H_2O/g of DNA vs relative humidity rises sharply at 88% for double-stranded DNA. The spectral data show that there is a significant phase transition in the vibrational state of the molecule between 88% and 92% RH. It is hypothesized that it is within this hydration interval that the molecule's available water binding sites become saturated with H_2O molecules. At higher hydration states, the molecule then begins to take the vibrational character of being in a solution-like state. Our most solution-like spectrum of the sample, at 98% RH, closely resembles that of a polynucleotide G·GC oligonucleotide triplex (Ouali *et al.*, 1993) in solution. Gravitimetric measurements of the hydrating triplex are planned.

The hydration-dependent glycosidic bond conformation has been monitored for the oligonucleotide G·GC triplex in the solid state. The data are consistent with the Neidle prediction that the bond adopts the *anti* conformation at high hydration states. The *syn* conformation was not evidenced, even in the 0% RH sample. Since neither of the traditional infrared marker bands for the glycosidic bond exist below 92% RH, the question arises: What is the infrared spectroscopic signature of the glycosidic bond in lower relative humidities?

The mid-infrared data presented here support the now commonplace conception that the conformations of DNA systems are polymorphic. In this triplex system, the canonical A and B conformations hardly play a traditional role, as evidenced by the existence of both C3′-*endo* and C2′-*endo* sugar puckers of $(dG)_{20}$·$(dG)_{20}(dC)_{20}$ at all relative humidities, particularly 0% RH. This is not to say, however, that remnants of the A to B transition with increased relative humidity do not exist. For example, the relative oscillator strengths of the modified 1239−1225-cm^{-1} band system follow the traditional pattern. Such polymorphic character is to be expected from a novel structure.

The following water association-dependent mid-infrared vibrations increase in oscillator strength with increasing relative humidity to 88% and then return to a lower absorption level at 92% RH: 1292 cm^{-1} (cytosine C6-NH_2 stretch), 1360 cm^{-1} (coupling of cytosine C6-NH_2, glycosidic linkage and furanose bond to the phosphodiester group), 1476 cm^{-1} (guanine C8-H bending), 1670 cm^{-1} (cytosine C6-NH_2 bend). Additional bands which increase in oscillator strength with increasing relative humidity are 1315, 1398, and 1625 cm^{-1}. It is hypothesized that all of these bands are related to the association of the triplex with water and that between the 88% and 92% hydration states a phase transition occurs wherein the molecule's environment shifts from a partially hydrated state to a hydration-saturated state.

Oscillator fits of important regions of the data are in progress. By quantitatively monitoring the hydration-dependent trends established here, refined assignments will be made to modes such as the 1696-cm^{-1} vibration. Potential energy distribution calculations for the G·GC triplex under a variety of hydration states are in progress (Chen & Prohofsky, 1994b). A comparison between the Lorentzian fits to our data and these theoretical predictions is planned in order to better comprehend the interaction between the triple-stranded nucleic acid and water.

REFERENCES

Akhebat, A., Dagneaux, C., Liqiuer, J., & Taillandier, E. (1992) *J. Biomol. Struct. Dyn. 10*, 577−588.

Chen, Y. Z., & Prohofsky, E. W. (1994a) *Phys. Rev. E49*, 873−881.

Chen, Y. Z., & Prohofsky, E. W. (1994b) Personal Communication.

Cooney, M., Czernuszewicz, G., Postel, E. H., Flint, S. J., & Hogan, M. E. (1988) *Science 241*, 456−459.

Duval-Valentin, G., Thuong, N. T., & Hélène, C. (1992) *Proc. Natl. Acad. Sci. U.S.A. 89*, 504−508.

Felsenfeld, G., Davies, D., & Rich, A. (1957) *J. Am. Chem. Soc. 79*, 2023−2034.

François, J.-C., Saison-Behmoaras, T., Thuong, N. T., & Hélène, C. (1989) *Proc. Natl. Acad. Sci. U.S.A. 86*, 9702−9706.

Ghomi, M., & Taillandier, E. (1985) *Eur. Biophys. J. 12*, 153−162.

Grigoriev, M., Praseuth, D., Robin, P., Hemar, A., Saison-Behmoras, T., Dautry-Varsat, A., Thuong, N. T., Hélène, C., & Harel-Bellan, H. (1992) *J. Biol. Chem. 267*, 3389−3395.

Ing, N. H., Beekman, J. M., Kessler, D. J., Murphy, M., Jayaraman, K., Zendegui, J. G., Hogan, M. E., O'Malley, B. W., & Tsai, M.-J. (1993) *Nucleic Acids Res. 21*, 2789−2796.

Laughton, C. A., & Neidle, S. (1992) *Nucleic Acids Res. 20*, 6535−6541.

Letellier, R., Ghomi, M., & Taillandier, E. (1986) *J. Biomol. Struct. Dyn. 3*, 671−687.

Lindsay, S. M., Lee, S. A., Powell, J. W., Weidlich, T., Demarco, C., Lewen, G. D., & Tao, N. J. (1988) *Biopolymers 27*, 1015−1043.

Liquier, J., Coffinier, P., Firon, M., & Taillandier, E. (1991) *J. Biomol. Struct. Dyn. 9*, 437−445.

Liu, K., Miles, H. T., Frazier, J., & Sasisekharan, V. (1993) *Biochemistry 32*, 11802−11809.

Maher, L. J., Dervan, P. B., & Wold, B. (1992) *Biochemistry 31*, 70−81.

McShan, W. M., Rossen, R. D., Laughter, A. H., Trial, J., Kessler, D. J., Zendegui, J. G., Hogan, M. E., & Orson, F. M. (1992) *J. Biol. Chem. 267*, 5712−5721.

Mohan, V., Smith, P. E., & Pettitt, M. B. (1993) *J. Am. Chem. Soc. 115*, 9297−9298.

Moser, H. E., & Dervan, P. B. (1987) *Science 238*, 645−650.

Ouali, M., Letellier, R., Sun, J. S., Akhebat, A., Adnet, F., Liquier, J., & Taillandier, E. (1993) *J. Am. Chem. Soc. 115*, 4264−4270.

Plum, G. E., Park, Y. W., Singleton, S. F., Dervan, P. B., & Breslauer, K. J. (1990) *Proc. Natl. Acad. Sci. U.S.A. 87*, 9436−9440.

Radhakrishnan, I., & Patel, D. J. (1994a) *Biochemistry 33*, 11405−11416.

Radhakrishnan, I., & Patel, D. J. (1994b) *Structure (London) 2*, 395−405.

Sfihi, H., Liquier, J., Urpi, L., Verdaguer, N., Subirana, J. A., Igolen, J., & Taillandier, E. (1993) *Biopolymers 33*, 1715−1723.

Shimanouchi, T., Tsuboi, M., & Kyogoku, Y. (1964) *Adv. Chem. Phys. 7*, 435−441.

Strobel, S. A., & Dervan, P. B. (1991) *Nature (London) 350*, 172−174.

Strobel, S. A., Stamm, L. A. D., Riba, L., Housman, D. E., & Dervan, P. B. (1991) *Science 254*, 1639−1642.

Taboury, J. A., Liquier, J., & Taillandier, E. (1985) *Can. J. Chem. 63*, 1904−1909.

Taillandier, E., & Liquier, J. (1992) *Methods Enzymol. 211*, 307−335.

Taillandier, E., Liquier, J., & Taboury, J. A. (1985) in *Advances in Infrared and Raman Spectroscopy* (Clark, R. H. J., & Hester, R. E., Eds.) Vol. 12, pp 65−114, Academic Press, Wiley-Heyden, New York.

Tsuboi, M., Kyogoku, Y., & Shimanouchi, T. (1962) *Biochim. Biophys. Acta 55*, 1−12.

BI942759R